

The LHCb Upgrade

H. Dijkstra*

CERN, CH-1211, Geneva 23, Switzerland

The LHCb detector has been designed to study CP violation and other rare phenomena in B-meson decays up to a luminosity of $\sim 5 \cdot 10^{32} \text{cm}^{-2} \text{s}^{-1}$. This paper will describe what is limiting LHCb to exploit the much higher luminosities available at the LHC, and what are the baseline modifications which will remedy these limitations. The aim of SuperLHCb is to increase the yields in hadronic B-decay channels by about a factor twenty compared to LHCb, while for channels with leptons in the final state a factor ten increase in statistics is envisaged.

I. INTRODUCTION

The LHCb experiment has been conceived to study CP violation and other rare phenomena in the B-meson decays with very high precision. The experiment is at the moment in the last phase of its construction, and is expected to be fully operational when the LHC machine will deliver its first pp collisions at 14 TeV in the summer of 2008. Figure 1 shows the layout of the detector, of which a detailed description can be found in [1]. The detector has been designed to be able to cope with an instantaneous luminosity up to $\sim 5 \cdot 10^{32} \text{cm}^{-2} \text{s}^{-1}$, and a total radiation dose corresponding to $\sim 20 \text{fb}^{-1}$. After an initial shake down of the detector in 2008, the aim is to look for New Physics (NP) signatures compatible with luminosities around $\sim 0.5 \text{fb}^{-1}$. The next four to five years, LHCb will accumulate $\sim 10 \text{fb}^{-1}$ to exploit the full physics program envisaged for the present detector. In the next section a selection will be presented of the expected performance of LHCb within the aforementioned luminosity range.

As mentioned above, LHCb will run at luminosities a factor 20-50 below the $10^{34} \text{cm}^{-2} \text{s}^{-1}$ design luminosity of the LHC. The machine optics of LHCb do allow to focus the beams sufficiently to run at luminosities a factor ten larger. Hence, the upgrade of LHCb is purely a question of the detector being able to profit from a higher peak luminosity. Section III will describe the conditions as a function of the delivered peak luminosity, and the limitations of LHCb to efficiently exploit an increase in luminosity.

The baseline upgrade scenario of the detector to SuperLHCb will be discussed in section IV, followed by expectations of yields for some selected physics channels in comparison with the proposed SuperKEKB performance in section V. The conclusions will be presented in section VI.

II. EXPECTED PERFORMANCE OF LHCb

The expected performance of LHCb is determined by generating pp interactions using the PYTHIA 6.2 generator [2], with the predefined option MSEL=2. To extrapolate to 14 TeV CM the value of the p_T^{min} parameter has been tuned as a function of energy to existing data [3]. The resulting charged track multiplicities in the acceptance of the spectrometer are $\sim 25\%$ larger than a similar tuning of CDF [4]. The particles are propagated through a detailed detector description using GEANT. Pileup in a bunch crossing, and spill-over from preceding and following bunches is included. Trigger studies have shown that the events written to storage are dominated by $b\bar{b}$ -events, hence all background is assumed to originate from $b\bar{b}$ -events, of which the equivalent of about 13 minutes of LHCb running have been fully simulated.

A. $\text{BR}(\text{B}_s \rightarrow \mu^+ \mu^-)$

The rare loop decay of $\text{B}_s \rightarrow \mu^+ \mu^-$ is sensitive to extensions of the Standard Model (SM) through loop corrections. Within the SM the decay rate has been computed [5] to be $\text{BR}(\text{B}_s \rightarrow \mu^+ \mu^-) = (3.4 \pm 0.4) 10^{-9}$. NP physics beyond the SM can increase this BR. In the minimal super-symmetric extension of the SM (MSSM) the BR increases as $\tan^6 \beta$, where $\tan \beta$ is the ratio of the Higgs vacuum expectation values. Hence, this makes the BR sensitive to models which prefer a relatively large $\tan \beta$. As an example figure 2 shows the expected BR as a function of the gaugino mass in the framework of a constrained minimal super-symmetric extension of the SM (CMSSM)[6]. The experimental challenge lies in the rejection of background, which is predominantly due to two muons which combine to form a good vertex with a signal mass. The muons originate either from semi-leptonic B-decays, or are due to misidentification of hadrons. LHCb combines a good invariant mass resolution, $\sigma(\text{M}_{\mu\mu}) \approx 20 \text{MeV}$, and excellent vertex resolution. In addition, the trigger can accept events with $p_T^\mu \geq 1 \text{GeV}$. Figure 3 shows the sensitivity [7] of $\text{BR}(\text{B}_s \rightarrow \mu^+ \mu^-)$ as a function of integrated luminosity. Within the first years of running LHCb

*for the LHCb collaboration

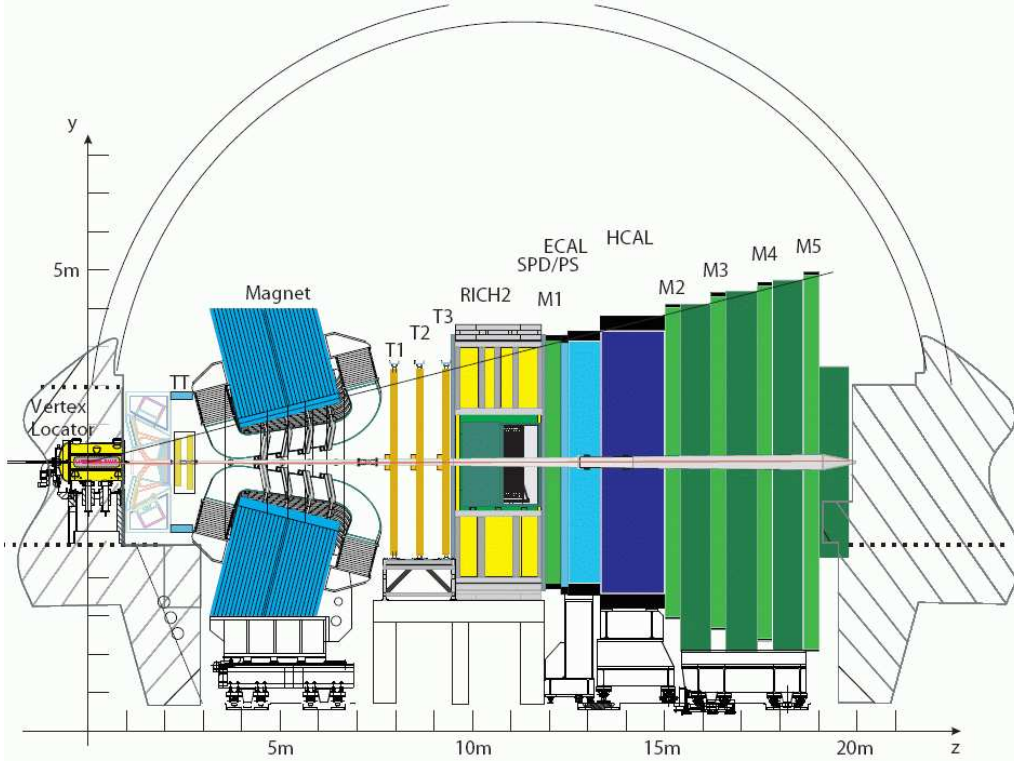


FIG. 1: LHCb detector layout, showing the Vertex Locator (VELO), the dipole magnet, the two RICH detectors, the four tracking stations TT, T1-T3, the Scintillating Pad Detector (SPD), Preshower (PS), Electromagnetic (ECAL) and Hadronic (HCAL) calorimeters, and the five muon stations M1-M5.

should be able to probe the whole CMSSM parameter space for large $\tan\beta$ values via this rare loop decay.

B. NP effects in $B \rightarrow K^*(K\pi)\mu^+\mu^-$

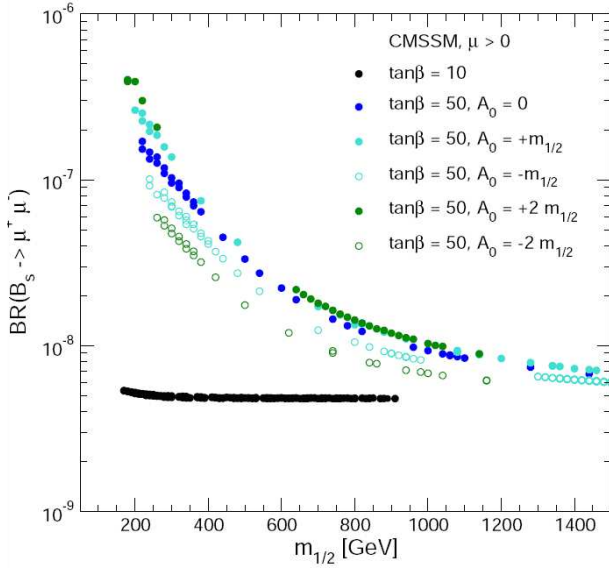


FIG. 2: The CMSSM prediction for $BR(B_s \rightarrow \mu^+\mu^-)$ as a function of the gaugino mass $m_{1/2}$ from [6].

While it is shown in the previous section that LHCb is very sensitive to NP effects at large $\tan\beta$ with a modest integrated luminosity, this section will explore the sensitivity to small $\tan\beta$ parameter space using the second transversity amplitude $A_T^{(2)}$ [8] in the decay $B \rightarrow K^*(K\pi)\mu^+\mu^-$. Figure 4 shows $A_T^{(2)}$ as a function of the dimuon mass for both the SM expectation, and for a representative choice of NP parameters, notably $\tan\beta = 5$, which do take into account the constraints from present observations. Note that the whole region between the shown NP curves and the SM are filled by solutions consistent with the constraints. The expected LHCb 95% confidence interval sensitivity for 10 fb^{-1} has been superimposed [9], assuming our measurements will fall precisely on the chosen NP expectation. While 10 fb^{-1} might allow to observe a hint of NP, an ten fold increase in statistic will allow a real observation of NP if nature has chosen this particular constellation.

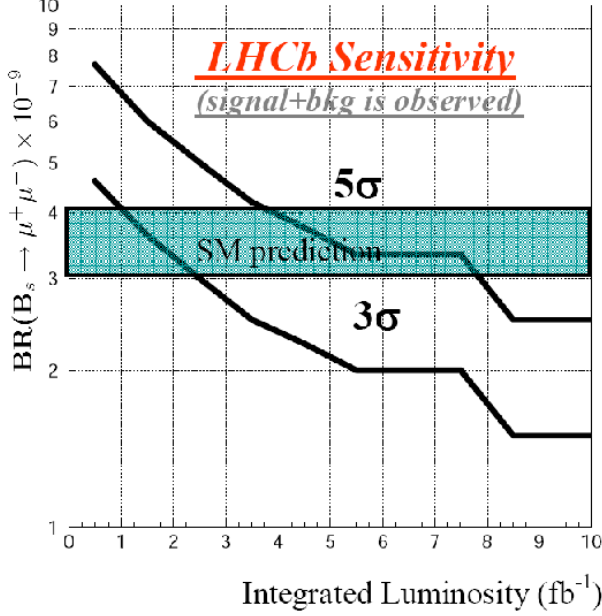


FIG. 3: The LHCb reach to observe (3σ) or discover (5σ) the $\text{BR}(B_s \rightarrow \mu^+ \mu^-)$ as a function of integrated luminosity.

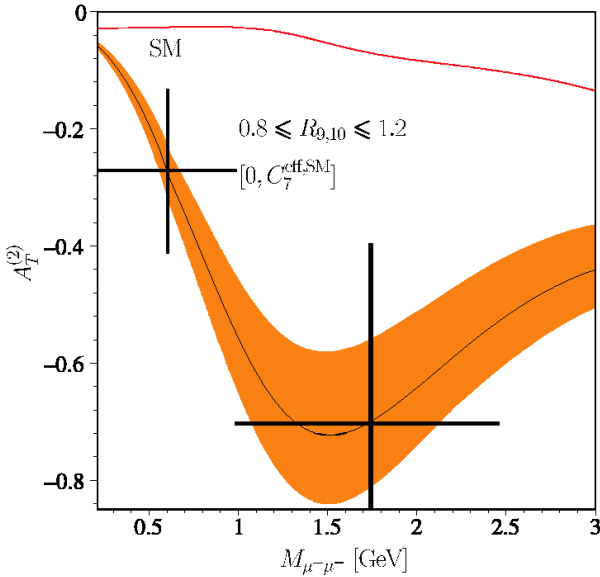


FIG. 4: $A_T^{(2)}$ as a function of the dimuon mass for the SM (top curve), and in the presence of NP contributions to the Wilson coefficients C_7 , C_9 and C_{10} as described in [8]. The data points indicate the expected 95% confidence level sensitivity of LHCb for an integrated luminosity of 10 fb^{-1} .

C. NP in $b \rightarrow s\bar{s}s$ transitions

Arguably the most intriguing hint of NP contributions to virtual loops in B-decays comes from the discrepancy between $\sin 2\beta$ measured in the time dependent CP asymmetries in $b \rightarrow c\bar{c}s$ and in $b \rightarrow s\bar{s}s$

transitions. The later cannot decay via a tree diagram in the SM, and hence is sensitive to NP contributions in its loop decay diagrams. The HFAG [10] averages for $\sin 2\beta(B \rightarrow J/\psi K_S^0) = 0.668 \pm 0.026$, and $\sin 2\beta^{\text{eff}}(B \rightarrow \phi K_S^0) = 0.39 \pm 0.18$. Although the discrepancy is not statistically significant, all $b \rightarrow s\bar{s}s$ show a value of $\sin 2\beta^{\text{eff}}$ which is lower than the tree counterpart. The expected sensitivity of LHCb for 10 fb^{-1} is $\sigma(\sin 2\beta^{\text{eff}}(B \rightarrow \phi K_S^0)) = \pm 0.14$, while B-factories for a combined integrated luminosity of 2 ab^{-1} expect an error of ± 0.12 in $\sin 2\beta^{\text{eff}}(B \rightarrow \phi K_S^0)$.

In addition LHCb has access to measuring the time dependent CP asymmetries in B_s -decays, which give access to the CP violating weak phase ϕ . While $\phi_d^{\text{SM}}(B \rightarrow J/\psi K_S^0) = 2\beta$, $\phi_s^{\text{SM}}(B \rightarrow J/\psi \phi) = 2\chi$, which is constrained to $-0.035 \pm_{0.006}^{0.014}$ by a fit to the unitary triangle within the SM [11]. NP in the $B_s \leftrightarrow \bar{B}_s$ mixing box diagram could enhance ϕ_s . With a modest integrated luminosity of 0.5 fb^{-1} LHCb is expected to reach a sensitivity of $\sigma(\phi_s(B_s \rightarrow J/\psi \phi)) = 0.046$ [12]. Already this sensitivity will constrain the parameters space of many extensions of the SM [13]. The golden hadronic counterpart is the decay $B_s \rightarrow \phi\phi$, which can only proceed via loop diagrams in the SM. In addition there is a cancellation of the B_s mixing and decay phase in the SM [14], which makes that $\phi_s(B_s \rightarrow \phi\phi) \approx 0$. The $\text{BR}(B_s \rightarrow J/\psi(\mu^+ \mu^-)\phi(K^+ K^-))$ is a factor eight larger than $\text{BR}(B_s \rightarrow \phi(K^+ K^-)\phi(K^+ K^-))$. In addition, as will be explained in the next section, this channel is much harder to trigger efficiently than channels with muons in the final state. As a consequence, LHCb expects $\sigma(\phi_s^{\phi\phi}) = 0.054$ [15] for an integrated luminosity of 10 fb^{-1} . Even a factor of twenty increase in statistics will result in an experimental error on $\phi_s^{\phi\phi}$ which is larger than the theoretical error.

III. THE LUMINOSITY UPGRADE

Before going into details about what is limiting the LHCb detector to already profit from day one from larger luminosities, what follows is a brief description of the experimental environment at the LHCb interaction point as a function of luminosity. As already mentioned in the introduction, the LHC machine has been designed to deliver a luminosity up to $10^{34} \text{ cm}^{-2} \text{ s}^{-1}$ at a General Purpose Detector (GPD). The optics around the LHCb interaction point (P8) allows LHCb to run at a luminosity up to 50% of the luminosity available at a GPD. Hence, the nominal LHC machine could deliver luminosities up to $5.10^{33} \text{ cm}^{-2} \text{ s}^{-1}$ at P8 [22]. The bunch crossing rate at P8 is given by the LHC machine to be 40.08 MHz, while 2622 out of the theoretically possible 3564 crossings [16] have protons in both bunches. Hence, the maximum rate of crossings with at least one pp interaction is ~ 30 MHz. The expected inelastic pp cross-section is 79.2

mb, of which 63 mb has at least two charged particles which can be reconstructed, the so-called visible cross-section. Figure 5 shows the number of crossings with at least one visible interaction and the mean number of visible interaction per crossing as a function of luminosity. Note that increasing the luminosity from

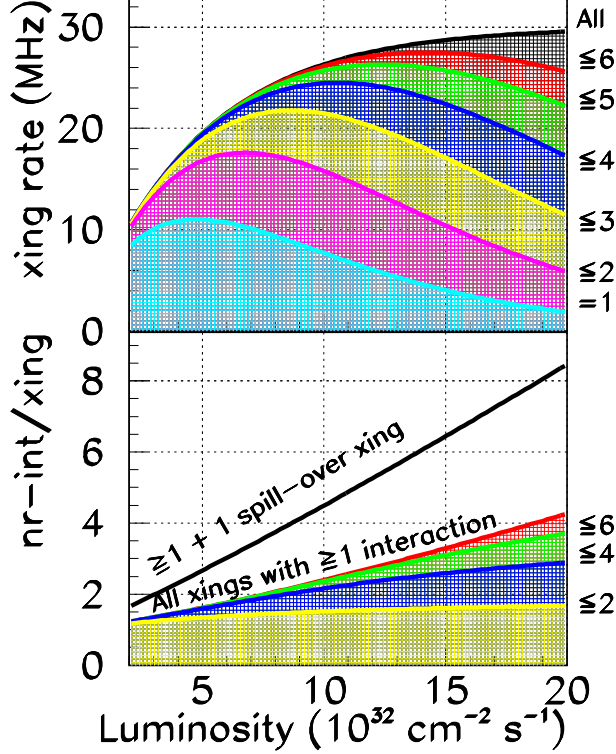


FIG. 5: Top plot shows the number of crossings with visible pp-interactions as a function of luminosity. The bottom plot shows the average number of visible pp-interactions per crossing, for events with at least one pp-interaction.

$(2 \rightarrow 10) \cdot 10^{32} \text{ cm}^{-2} \text{ s}^{-1}$ will only increase the mean number of interactions per crossing by a factor two, since the number of crossings with at least one interaction increases from $10 \rightarrow 26$ MHz. While the increase in occupancy for detectors which are only sensitive to pileup is minimal, spill-over increases linearly with luminosity as is indicated in the bottom plot of figure 5.

A. The LHCb Trigger

LHCb has a two level trigger system, called Level-0 (L0) and the High Level Trigger (HLT). L0 is a trigger implemented in hardware, and its purpose is to reduce the rate of crossings with interactions to below a rate of 1.1 MHz. This is the maximum rate at which all LHCb data can be readout by the front-end (FE) electronics. L0 reconstructs the highest E_T hadron, electron and photon, and the two highest p_T

muons. It triggers on events with a threshold of typically $E_T^{\text{hadron}} \gtrsim 3.5$ GeV, $E_T^{e,\gamma} \gtrsim 2.5$ GeV, and $p_T^\mu \gtrsim 1$ GeV at $2 \cdot 10^{32} \text{ cm}^{-2} \text{ s}^{-1}$. Figure 6 shows the yield of L0-triggered events, normalized to their yield at $2 \cdot 10^{32} \text{ cm}^{-2} \text{ s}^{-1}$ as a function of the luminosity for a leptonic and a hadronic B-decay channel. The L0-

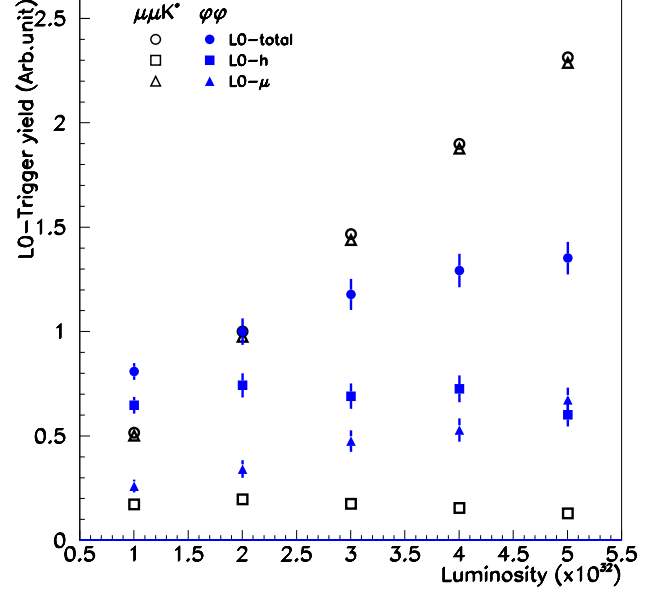


FIG. 6: The L0-trigger yield as a function of luminosity for two decay channels: $\mu\mu K^*$ (open points) and $\phi\phi$ (closed points). The total L0-trigger yield, and the contributions from the L0-hadron and muon triggers are shown separately.

hadron trigger absorbs $\sim 70\%$ of the L0 bandwidth at $2 \cdot 10^{32} \text{ cm}^{-2} \text{ s}^{-1}$, and its threshold is already larger than half the B-mass. The increase in mainly the rate of visible pp interactions requires an increase in the threshold, and the resulting loss in efficiency nullifies the increase in luminosity, resulting in an almost constant yield for the hadron trigger. Contrary, the muon trigger absorbs only $\sim 15\%$ of the available bandwidth at $2 \cdot 10^{32} \text{ cm}^{-2} \text{ s}^{-1}$, at which rate it already has an efficiency around 90% for leptonic B-decays. For larger luminosities the loss in efficiency is minor, showing an almost linear dependence of its yield on luminosity. Note that at a luminosity of $5 \cdot 10^{32} \text{ cm}^{-2} \text{ s}^{-1}$ about half the yield in $B_s \rightarrow \phi\phi$ is due to the muon trigger on the leptonic decay of the tagging B.

After L0, all detectors are readout, and full event building is performed on the CPU nodes of the Event Filter Farm (EFF). The HLT consists of a C++ application which is running on every CPU of the EFF, which contains between 1000 and 2000 multi-core computing nodes. Each HLT application has access to all data in one event, and thus in principle could be executing the off-line selection algorithms, which would render it a 100% trigger efficiency by definition. But given the 1 MHz output rate of L0 and the

limited CPU power available, the HLT aims at rejecting the bulk of the events by using only part of the full information which is available. The HLT starts with so-called alleys, where each alley addresses one of the trigger types of the L0-trigger, enriching the B-content of the events by refining the L0 objects, and adding impact parameter information. If an event is selected by at least one alley, it is processed by the inclusive triggers, where specific resonances are reconstructed and selected, and the exclusive triggers, which aim to fully reconstruct B-hadron final states. Events will be written to storage with a rate of ~ 2 kHz.

As is shown in figure 6, even hadronic B-decays receive a considerable fraction of their L0 efficiency due to the muon trigger which is usually fired by a leptonic decay of the opposite B. Hence, in the 2 kHz output rate about half is reserved for events with a large p_T muon with a significant impact parameter. Simulation shows that 900 Hz of single muon triggers contain ~ 550 Hz of true $B \rightarrow \mu X$ decays. Figure 7 illustrates the yield of B-decays, of which the decay products are fully contained in the LHCb acceptance, while the event is triggered on the semi-leptonic B-decay of the other B-hadron. It shows the correlation of the $B\bar{B}$ -pair in pseudo rapidity, which makes that when the lepton from a semi-leptonic decay of one of the B-mesons is in the acceptance of LHCb, there is a 30 – 40% probability that all the decay product of the opposite B are also contained in the spectrometer. Hence, just the inclusive muon trigger will already provide a rate of $\sim 10^9/\text{fb}^{-1}$ fully contained B-decays, with a tagging performance of $\epsilon D^2 \approx 0.15$ due to the presence of a large p_T muon.

The typical efficiency of the whole trigger chain for hadronic, radiative and leptonic B-decays is 25-30%, 30-40% and 60-70% respectively. An upgrade of the trigger should not only be able to cope with larger luminosities, but should be designed to at least gain a factor two for hadronic B-decays like $B_s \rightarrow \phi\phi$.

B. Tracking and Particle Identification

The tracking of LHCb commences by reconstructing all tracks inside the VELO. The VELO is based on silicon (Si)-sensors, and the channel occupancy at $2.10^{32} \text{ cm}^{-2}\text{s}^{-1}$ is $\sim 1\%$, which is kept roughly constant as a function of the radius due to the layout of the strips. This occupancy increases to $\sim 3\%$ at $2.10^{33} \text{ cm}^{-2}\text{s}^{-1}$. As a result the tracking performance [17] in the VELO loses only 2.7% in efficiency for this factor ten increase in luminosity, while using reconstruction code tuned for the low luminosities. This is as expected from figure 5, since the VELO electronics has a limited sensitivity to spill-over, and as a consequence only 27% of its hits at $2.10^{33} \text{ cm}^{-2}\text{s}^{-1}$ are due to spill-over.

To assign momentum to the VELO tracks, every

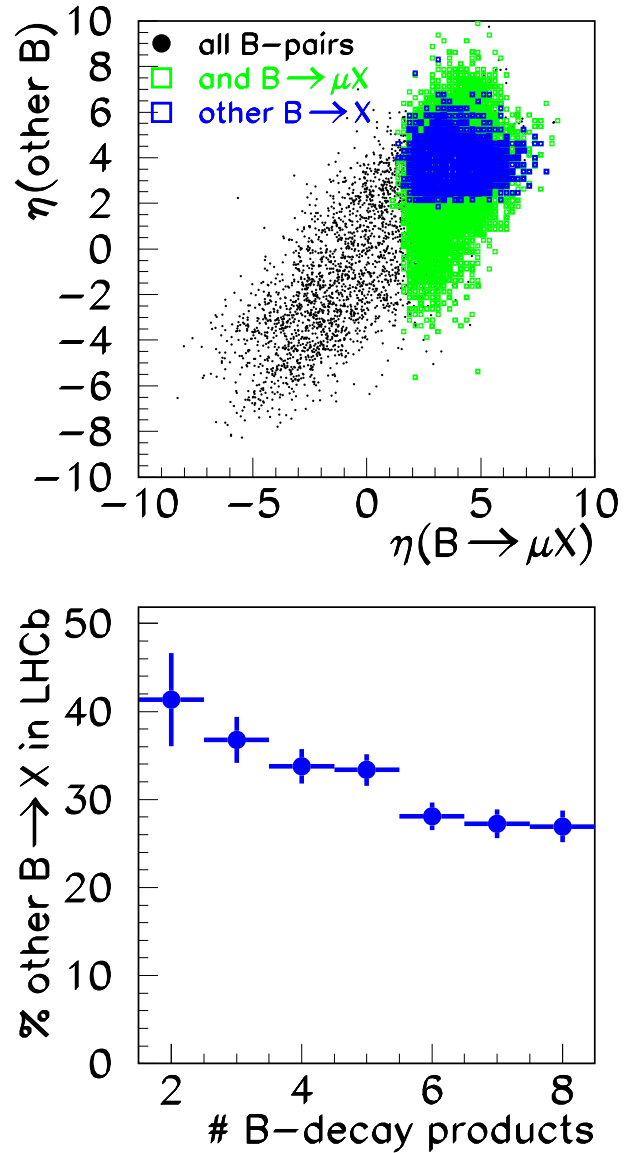


FIG. 7: Top plot shows the pseudo rapidity (η) correlation of a $B\bar{B}$ -pair. Of all the produced $B\bar{B}$ -pairs (black dots), the single muon trigger selects the pairs of which one B has its decay-muon inside the acceptance of LHCb (green squares). The blue squares indicate the rapidity of the other B, if all its decay products are inside the LHCb acceptance. The bottom plot shows the fraction of “other” B-decays in the LHCb acceptance as a function of the number of B-decay products.

track is combined with a hit in the T-stations, located behind the magnet, in turn. Around the trajectory defined by the VELO track and a T-hit, a search is performed in the other tracking stations including TT. In addition there is also a stand-alone pattern recognition performed in the T-stations, mainly to recover K_S^0 which decay behind the VELO. The outer part of the T-stations (OT) are constructed of 5 mm diameter straws, with a drift-time up to 50 ns. Including

the effect of the length of the 2.4 m long wires, this requires a readout gate of three consecutive crossings to obtain the maximum efficiency. As a consequence, the OT occupancy rises from $6 \rightarrow 25\%$ for a ten-fold luminosity increase from $(2 \rightarrow 20) \cdot 10^{32} \text{ cm}^{-2}\text{s}^{-1}$. At $2 \cdot 10^{33} \text{ cm}^{-2}\text{s}^{-1}$ 60% of the OT hits are due to spill-over. Both TT and the inner part of the T-stations (IT) are made of Si-sensors. At $2 \cdot 10^{33} \text{ cm}^{-2}\text{s}^{-1}$ 44(25)% of the TT(IT) hits are due to spill-over.

The tracking performance as a function of luminosity is shown in figure 8. Above a luminosity of

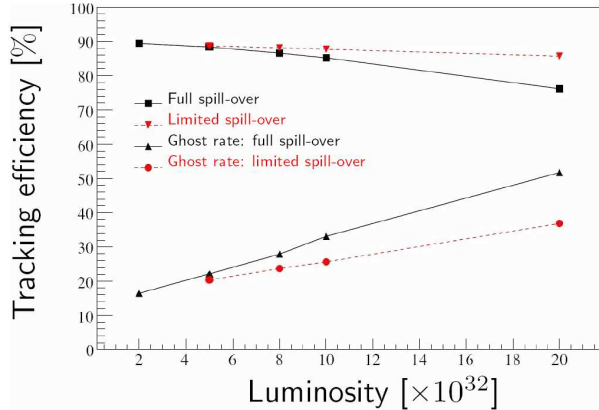


FIG. 8: The tracking efficiency as a function of luminosity. Limited spill-over uses the same spill-over as obtained at a luminosity of $2 \cdot 10^{32} \text{ cm}^{-2}\text{s}^{-1}$, irrespective of the luminosity.

$5 \cdot 10^{32} \text{ cm}^{-2}\text{s}^{-1}$ the difference between the tracking performance with full spill-over and a spill-over equivalent to the spill-over at $2 \cdot 10^{32} \text{ cm}^{-2}\text{s}^{-1}$ is clearly visible. The per track loss in tracking efficiency from $(2 \rightarrow 10) \cdot 10^{32} \text{ cm}^{-2}\text{s}^{-1}$ is $\sim 5\%$, which is a small price to be paid, even for a 4-prong decay, compared to the factor 5 increase in luminosity. However, an additional increase of a factor two in luminosity would result in a loss of 36% of the 4-prong decays, hence would almost eliminate the additional factor two increase.

The electronics of the RICH detector is virtually insensitive to spill-over. The increase in occupancy for an event with a $B\bar{B}$ -pair and its pileup events is only a factor 2.5 for the factor ten increase in luminosity to $2 \cdot 10^{33} \text{ cm}^{-2}\text{s}^{-1}$. This is even a smaller increase than shown in figure 5, since pp-interactions producing a $B\bar{B}$ -pair cause about twice the occupancy compared to visible pp-interactions. The efficiency to positively identify a kaon degrades by 10% for the 10 fold increase in luminosity. The loss is dominated by the degradation of the RICH1 performance, which has the higher backgrounds and occupancies. In the above simulation the effect of inefficiency due to overflowing buffers at high occupancy has not been taken into account, since it will be argued in the next section that

the front-end electronics will have to be replaced to allow the trigger to be upgraded.

The muon chambers and the calorimeters both have negligible sensitivity to spill-over, and hence the increase in occupancy follows the same trend as that of the RICH. Their performances development as a function of luminosity is more related to dead time inefficiency and radiation damage, rather than occupancy per bunch crossing. These effects are not simulated in the MC, and hence no reliable performance as a function of luminosity is available.

IV. THE SUPERLHCb DETECTOR

In the previous section it was shown that the subsystem of LHCb which does not scale in performance with an increased luminosity is the trigger, and in particular the trigger for hadronic B-decays which will not be able to retain its efficiency for larger luminosities. Since the trigger efficiency for hadronic B-decays is expected to be 25 – 30%, the goal of an upgrade of the trigger should also be to improve on the hadron trigger efficiency by at least a factor two. At 14 TeV center of mass pp collisions $\sigma_{b\bar{b}}$ is assumed to be $500 \mu\text{b}$. Hence, with a luminosity of $2 \cdot 10^{33} \text{ cm}^{-2}\text{s}^{-1}$ there will be 10^6 $b\bar{b}$ -pairs produced in the LHCb interaction point per second, of which 43% will have at least one B-hadron with a polar angle below 400 mrad, i.e. pointing in the direction of the spectrometer. Hence, an efficient and selective trigger should already at a very large rate be able to distinguish between wanted and unwanted B-decays. Pilot studies on improving the trigger all show that the only way to be able to provide adequate selectivity of the trigger, and maintain large efficiency for hadronic B-decays is to be able to measure both the momentum and impact parameter of B-decay products simultaneously.

The present FE-architecture imposes that the detectors which do not participate in the L0-trigger can only be read-out with a maximum event rate of 1.1 MHz, and that the L0-latency available for making the L0 decision, which is now $1.5 \mu\text{s}$, can be stretched to a few μs at most. The algorithms required to efficiently select B-decays require latencies far superior to what is available with the present architecture.

Hence, SuperLHCb has opted for a FE-architecture which requires all sub-detectors to read-out their data at the full 40 MHz rate of the LHC machine. The data should be transmitted over optical fibers to an interface board (TELL40 [18]) between the FE and a large EFF. The trigger algorithm is then executed on the EFF, much like the present HLT. Technology tracking estimates show that by 2013 SuperLHCb should be able to acquire sufficient CPU power to be able to perform a HLT like trigger on a large CPU farm. However, in case the EFF at the start of SuperLHCb would be undersized, the TELL40 boards will be equipped

with a throttle to prevent buffer overflows. This throttle should also include an event selection much like the present L0, based on the data available in the TELL40 boards, to enrich rather than just pre-scale events. At a luminosity of $6.10^{32} \text{ cm}^{-2}\text{s}^{-1}$ and an assumed CPU power able to process 5 MHz of events, the trigger efficiency is 66% for the channel $B_s \rightarrow D_s^\mp K^\pm$. For this simulation the throttle requires at least one HCAL-cluster with $E_T^{\text{hadron}} > 3 \text{ GeV}$, which has an efficiency of 76% for this signal. Note that a 2 GeV requirement would correspond to 10 MHz of input rate into the EFF, while it would increase the efficiency from $76 \rightarrow 95\%$ at the start of the EFF, while with LHCb running at $2.10^{32} \text{ cm}^{-2}\text{s}^{-1}$ the equivalent efficiency for this channel at the start of the HLT is only 39%.

The upgraded FE-architecture requires that the FE-electronics of all sub-detectors needs to be replaced, with the exception of the muon chambers which already have the 40 MHz capability. The Si-detectors, which cover the areas close to the beam, will suffer from a five fold increase in allowed radiation dose, and hence need to be replaced by more radiation resistant technologies. For the RICH the photon detection and the FE-electronics is combined in a Hybrid Photo Detector, which needs to be replaced entirely. The OT requires the replacement of its FE-boards. Running these detectors with a slightly faster gas, combined with taking advantage of being able to pre-process spill-over in the TELL40 boards could reduce the occupancy from $25 \rightarrow 17\%$ at $2.10^{33} \text{ cm}^{-2}\text{s}^{-1}$. This could be combined with enlarging the coverage of IT, to reduce the occupancy close to the beam even further. The M1 muon chamber, which is located just before the Calorimeter, would suffer from a too high occupancy, and will be removed. It now serves to provide an improved momentum measurement in L0, which will no longer be necessary. The resolution in the inner part of the Calorimeter will degrade with radiation. It will have to be replaced with a more radiation tolerant technology. This might also allow LHCb to extend the calorimeter coverage down to $\eta = 5$ from the present maximum pseudo rapidity of 4.2, i.e. an increase in coverage of 25%. Last but not least, all results presented from simulation studies did not attempt to adapt the algorithms to a higher occupancy environment, hence they are considered to be conservative.

V. PROJECTED YIELDS OF SUPERLHCb

The LHC machine schedule assumes that first collisions at 14 TeV will be delivered in the summer of 2008. The top plot of figure 9 shows the expected integrated luminosity profile, which assumes that LHCb will run at $(2-5).10^{32} \text{ cm}^{-2}\text{s}^{-1}$, and that the machine and experiment will only slowly ramp up to the full capability in 2011.

LHCb would then run at maximum luminosity for two years, and then have a one year shutdown to change over to the new FE-architecture in 2013. In 2014 it assumes to run at half of its full capability, after which it accumulates 20 fb^{-1} per year for the rest of the next decade.

For comparison the running scenario of the proposed SuperKEKB [19] is shown in the same plot. The closed squares (open circles) show the information of LHCb (KEKB). The middle and bottom plots show the expected yield for $B \rightarrow K^* \mu\mu$, $B_s \rightarrow \phi\phi$ and $B \rightarrow \phi K_S$ after trigger and strict off-line selection to obtain a good Background/Signal ratio. For the channels which require tagging to perform the time dependent CP asymmetry analysis, the yield has been multiplied by the effective tagging efficiency ϵD^2 , 0.07 and 0.3 for LHCb and KEKB respectively, to take into account the better tagging performance at a B-factory.

VI. CONCLUSIONS

The last few years have seen an impressive progress in precision measurements of B-decays, notably from the B-factories and the Fermilab collider. The remarkable agreement between CP conserving and violating observables indicates that the main source of CP-violation can be attributed to the KM-mechanism [20]. In their quest for discovering NP, the new generation of experiments have to be able to detect small deviations from the SM, which requires increasingly larger data sets. LHCb is nearing the end of its construction, and will be ready to look for NP with a projected integrated luminosity of around 10 fb^{-1} in the years to come. This paper describes the way LHCb can be upgraded to be able to have access to NP even beyond the possibilities of the first phase of LHCb.

The main component of LHCb which limits it to profit from the available nominal luminosity of the LHC machine is the hadron-trigger. Consequently SuperLHCb will have a new FE-architecture and trigger which aims at being able to cope with luminosities around $2.10^{33} \text{ cm}^{-2}\text{s}^{-1}$, and which will have a hadron trigger efficiency twice larger than the present trigger, resulting in a twenty fold increase in hadronic B-decays available for analysis. In addition, the leptonic decay channels will profit from an increase in luminosity at least linearly.

Acknowledgments

This paper would not have been possible without the work done by many of my colleagues in LHCb, notably those who contributed to the “1st LHCb Collaboration Upgrade Workshop” [21]. I would like to

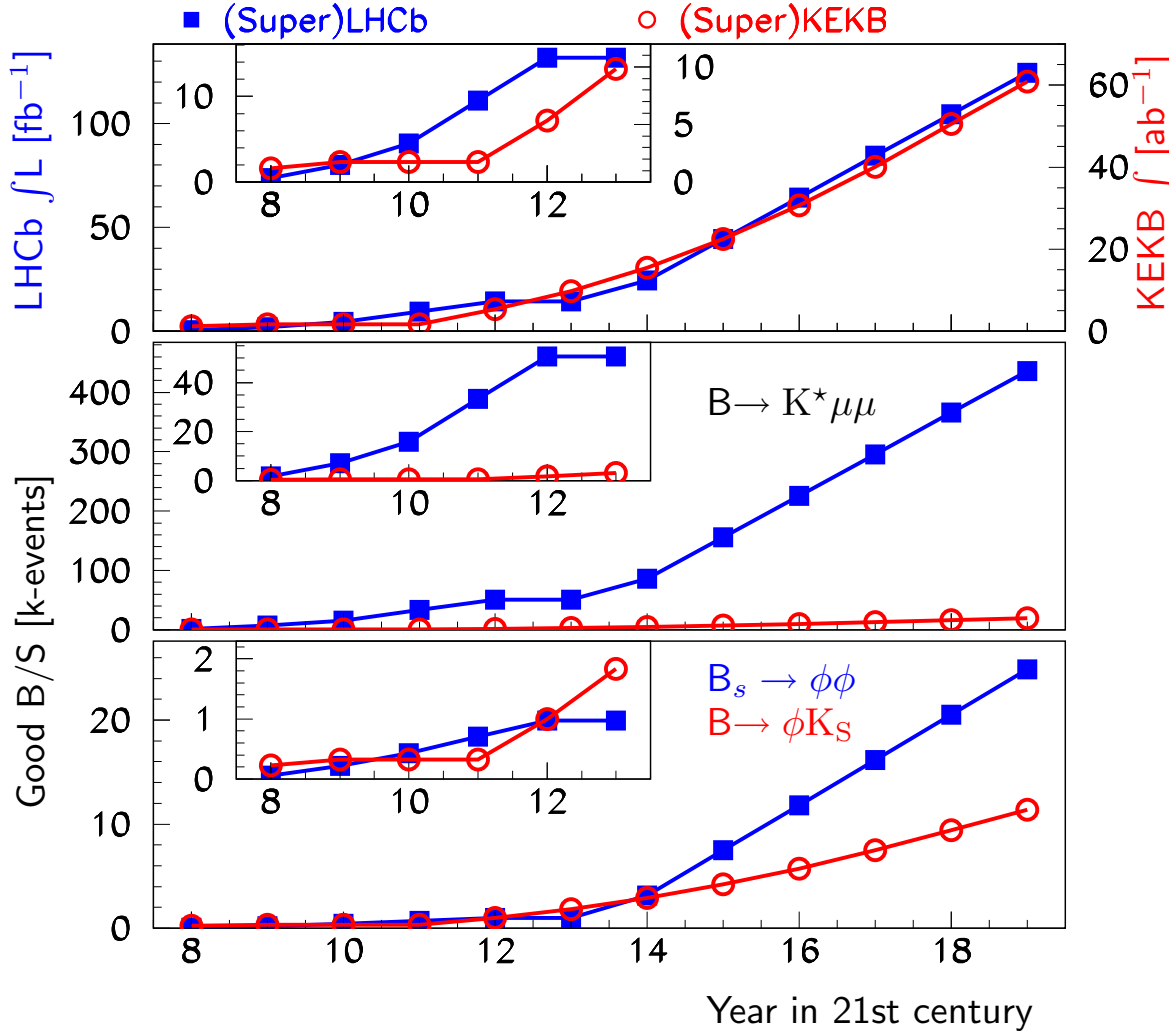


FIG. 9: Top plot shows the projected integrated luminosity for LHCb and Super LHCb, compared to (Super)KEKB. The middle and bottom plots show the expected yield for the channels indicated, after trigger and strict off-line selection to obtain a good Background/Signal ratio. The yield of $B_s \rightarrow \phi \phi$ and $B \rightarrow \phi K_S$ has been multiplied by ϵD^2 , 0.07 and 0.3 for LHCb and KEKB respectively, to take into account the better tagging performance at a B-factory.

thank them all. I would like to thank Franz Muheim for carefully reading the manuscript.

-
- [1] LHCb collaboration, R. Antunes Nobrega *et al.*, LHCb Reoptimized Detector Design and Performance, CERN-LHCC/2003-030.
 - [2] T. Sjöstrand *et al.*, Computer Physics Commun. **135** (2001) 238.
 - [3] P. Bartalini *et al.*, LHCb 1999-028.
 - [4] CDF Collaboration, D. Acosta *et al.*, Phys. Rev. D **65** (2002) 072005.
 - [5] A.J. Buras, Phys Lett. B **566** (2003) 115.
 - [6] J. Ellis *et al.*, hep-ph/0411216.
 - [7] D. Martinez *et al.*, LHCb 2007-033.
 - [8] F. Krüger and J. Matias, hep-ph/0502060.
 - [9] E. Lunghi and J. Matias, hep-ph/0612166.
 - [10] U. Egede, LHCb2007-057.
 - [11] Heavy Flavour Averaging Group, <http://www.slac.stanford.edu/xorg/hfag/triangle/moriond2007/>.
 - [12] J. Charles *et al.*, CKMfitter Group, Eur. Phys. J. C **41**, 1-131 (2005) [hep-ph/0406184], and updated results at this conference.
 - [13] P. Vankov, LHCb 2007-065.
 - [14] Z. Ligeti *et al.*, hep-ph/0604112.
 - [15] M. Raidal, Phys. Rev. Lett. **89**, 231803 (2002).
 - [16] S. Amato *et al.*, LHCb 2007-047.

- [16] J. Christiansen, LHCb 2001-014
- [17] M. Needham, LHCb 2007-021
- [18] A successor of the board described in: F. Legger *et al.*, LHCb 2004-100, which is able to cope with 40 MHz event rate.
- [19] Taken from M. Hazumi, B factories: status and prospects, Flavour in the era of the LHC, March 2007, <http://mlm.home.cern.ch/mlm/FlavLHC.html>
- [20] M. Kobayashi and T. Maskawa, Prog. Theor. Phys. **49** (1973) 652.
- [21] “1st LHCb Collaboration Upgrade Workshop”, January 2007, Edinburgh: <http://indico.cern.ch/conferenceDisplay.py?confId=8351>.
- [22] While the nominal LHC is sufficient for the LHCb upgrade, there is a proposal to increase the nominal lu-

minosity of the machine to $8.10^{34} \text{ cm}^{-2} \text{ s}^{-1}$, the SLHC, around the middle of the next decade. The bunch separation for LHCb will remain 25 ns, but there are two schemes to fill the bunches. The preferred scheme will use large currents in the even bunches, and low current in the odd bunches. Since P8 is displaced relative to the GPD interaction points by 1.5 bunch spacings, it will result in colliding odd with even bunches in P8. In the GPD collision points the collisions are odd×odd and even×even. This will allow LHCb to choose its luminosity using the current in the odd bunches. A GPD will ignore the odd×odd interactions, since it will contribute a luminosity at least a factor 400 smaller than what is obtained in the even×even collisions.